Stimulation of frontal pathways disrupts hand muscle control during object manipulation

Luca Viganò,[1,†] Henrietta Howells,[2,†] Marco Rossi,[1] Marco Rabuffetti,[3] Guglielmo Puglisi,[1,2] Antonella Leonetti,[1] Andrea Bellacicca,[2] Marco Conti Nibali,[1] Lorenzo Gay,[1] Tommaso Sciortino,[1] Gabriella Cerri,[2] Lorenzo Bello[1] and Luca Fornia[2]

[†]**These authors contributed equally to this work.**

Abstract

The activity of frontal motor areas during hand-object interaction is coordinated by dense communication along specific white matter pathways. This architecture allows the continuous shaping of voluntary motor output and, despite extensively investigated in non-human primate studies, remains poorly understood in humans. Disclosure of this system is crucial for predicting and treatment of motor deficits after brain lesions.

For this purpose, we investigated the effect of direct electrical stimulation on white matter pathways within the frontal lobe on hand-object manipulation. This was tested in thirty-four patients (15 left hemisphere, mean age 42 years, 17 male, 15 with tractography) undergoing awake neurosurgery for frontal lobe tumour removal with the aid of the brain mapping technique. The stimulation outcome was quantified based on hand-muscle activity required by task execution. The white matter pathways responsive to stimulation with an interference on muscles were identified by means of probabilistic density estimation of stimulated sites, tract-based lesion-symptom (disconnectome) analysis and diffusion tractography on the single patient level. Finally, we assessed the effect of permanent tracts disconnection on motor outcome in the immediate postoperative period using a multivariate lesion-symptom mapping approach.

The analysis showed that stimulation disrupted hand-muscle activity during task execution in 66 sites within the white matter below dorsal and ventral premotor regions. Two different EMG interference patterns associated with different structural architectures emerged: 1) an *arrest* pattern, characterised by complete impairment of muscle activity associated with an abrupt task interruption, occurred when stimulating a white matter area below the dorsal premotor region. Local mid-U-shaped fibres, superior fronto-striatal, corticospinal and dorsal fronto-parietal fibres intersected with this region. 2) a *clumsy* pattern, characterised by partial disruption of

muscle activity associated with movement slowdown and/or uncoordinated finger movements, occurred when stimulating a white matter area below the ventral premotor region. Ventral fronto-parietal and inferior fronto-striatal tracts intersected with this region. Finally, only resections partially including the dorsal white matter region surrounding the supplementary motor area were associated with transient upper-limb deficit (p=0.05; 5000 permutations).
Overall, the results identify two distinct frontal white matter regions possibly mediating different aspects of hand-object interaction via distinct sets of structural connectivity. We suggest the dorsal region, associated with arrest pattern and post-operative immediate motor deficits, to be functionally proximal to motor output implementation, while the ventral region may be involved in sensorimotor integration required for task execution.

Author affiliations:
1 Neurosurgical Oncology Unit, Department of Oncology and Hemato-Oncology, Università degli Studi di Milano
2 MoCA Laboratory, Department of Medical Biotechnology and Translational Medicine, Universita`degli Studi di Milano
3 Biomedical Technology Department, IRCCS Fondazione Don Carlo Gnocchi ONLUS, Milano, Italy

Correspondence to: Gabriella Cerri
Department of Medical Biotechnology and Translational Medicine, Universita`degli Studi di Milano, Via Fratelli Cervi, 93 – Segrate, 20090 (MI), USA
E-mail: gabriella.cerri@unimi.it

Running title: Frontal tracts in hand motor control

Keywords: intraoperative brain mapping; EMG; object manipulation; diffusion tractography; hand motor control

Abbreviations: aCC = autocorrelation coefficient; AF = arcuate fasciculus; DES = direct electrical stimulation; EOR = extent of resection; FAT = frontal aslant tract; HARDI = high angular resolution diffusion imaging; HMt = hand-manipulation task; Inf_FST = inferior fronto-striatal tract; M1 = primary motor area; Mid-U = middle U-shaped fibres; PDE = probability density estimation; RMS = root mean square; SLF = superior longitudinal fasciculus; M1-CST = primary motor area corticospinal tract; dPM-CST = dorsal premotor

area corticospinal tract; vPM-CST = ventral premotor area corticospinal tract; SMA-CST = Supplementary motor area corticospinal tract; Sup_FST = superior fronto-striatal tract; SVR-LSM = support vector regression lesion symptom mapping.

Introduction

The ability to manipulate objects is a key behaviour that allows humans to interact with their environment. Humans have particularly refined dexterity over other non-human primates, due to the unique structure of their hands[1] and the high density of direct projections from the primary motor cortex (M1) to spinal motoneurons[2]. To generate the adequate descending motor command, premotor areas and direct-indirect cortico-thalamic loops act in parallel to refine multiple aspects, from movement planning, selection, sequencing and inhibition to sensorimotor transformations and on-line updating of the motor program.[3–8] The orchestrated activity of these networks is supported by specific white matter projections.[9–14] In humans, these pathways have been anatomically described[15], however their role in controlling hand muscles during object manipulation has never been directly tested by means of an invasive electrophysiological approach. A comprehensive description of the connectional anatomy of motor control is still lacking in comparative functional neuroanatomy[16] but seems crucial for clinical practice from surgical interventions to neurorehabilitation.[17,18]

To this aim, the integration between intraoperative direct electrical stimulation (DES), with its direct access to the functional role of white matter sites during brain mapping[19–21], and diffusion tractography, which can model white matter connections, represents one of the most promising approaches in humans. Recent developments in diffusion tractography enables the investigation of white mater pathways at high resolution[22] and the visualisation of fronto-parietal fibres crucial for motor control[23,24]. In cases where tractography has not been performed, tract-based lesion-symptom analysis using the 'disconnectome' approach generates probabilistic maps of connections from a given region of interest, such as a functionally eloquent stimulation site, enabling the consideration of a stimulation effect as the result of a disconnection within a wider network.[9,25]

In the context of intraoperative brain mapping for tumour removal, we recently demonstrated that stimulation of distinct precentral cortical sectors during the execution of an haptically-driven hand-object manipulation task (HMt) interferes with muscle activity with distinguishing

features. This suggested that DES, applied while performing a specific hand motor task coupled with electromyographic recording, may reveal areas mediating different aspects of motor control possibly via distinct networks[26–29] .

Within the same clinical context and with the same stimulation paradigm, we here investigate the anatomo-functional organization of white matter below premotor areas during the same task. To this aim, we assessed whether subcortical DES caused interferences in hand muscle patterns during the HMt in thirty-six patients undergoing awake surgery for removal of a brain tumour. Quantitative analysis of muscle activity affected at eloquent sites and their anatomical distribution were assessed using a spatial probability methodology developed in previous studies.[21,26,28] We evaluated the affected white matter tracts for each patient by using a disconnectome approach[25] for different stimulation effects based on HARDI tractography of healthy subjects acquired by the Human Connectome Project (7T protocol). We refined this result in a subset of fifteen patients that underwent preoperative diffusion tractography, using their unique intraoperative stimulation site and white matter tractogram. Finally, to investigate whether postoperative motor deficits were associated with resection of a specific white matter region, we performed a support vector regression lesion-symptom mapping (SVR-LSM) using patients' post-operative resection cavities (n=34). In the subset of patients with diffusion tractography (n=15), the postoperative motor outcome was correlated with the percentage of disconnection for different white matter tracts. This is a novel study combining electrophysiological and structural neuroimaging to directly investigate frontal white matter recruited during object manipulation. A flowchart of the methods adopted in the study is shown in Figure 1. The results are discussed in light of hodological and electrophysiological evidence in non-human primate investigating hand-related pathways. A more thorough appreciation of the anatomo-functional organization and functional properties of this network is crucial for a safe and effective resection of tumours involving this area.

Methods

Study design and patient cohort

Thirty-four patients that were candidates for an awake neurosurgical resection for a left (n=15) or right (n=19) hemisphere brain tumour at the Surgical Neuro-oncology Unit (of author L.B) between 2016 and 2019 (Table 1) were studied. All participants gave written informed consent

to the surgical mapping procedure (IRB1299) and data analysis for research purposes, following the principles outlined in the Declaration of Helsinki. The study was performed with strict adherence to the clinical procedure for tumour removal. Patients were included if they fulfilled the following criteria: no preoperative motor deficits, no long-term history of epilepsy and no previous neurosurgical needle or open biopsy, no tumour infiltration of the tested area. All patients were assessed for handedness using the Edinburgh Handedness Inventory and underwent a pre-operative, 5-day and 1-month postoperative neuropsychological evaluation of cognitive ability and neurological examinations of motor ability[30]. Surgical resection was aimed at supratotal resection[31], involving at the posterior border of the resection cavity the connectivity in the tested area.

Intraoperative subcortical brain mapping for object manipulation

Surgery was performed using asleep-awake-asleep anaesthesia, with the aim to identify pure motor (fibres origination from M1), praxis (see below), language, visual and cognitive boundaries[21,32–34]. For praxis mapping during tumour resection, low frequency DES (LF-DES) delivered by a bipolar probe with a 5mm distance tip (60 Hz, pulse width=0,5ms, biphasic current, 1-4 seconds of stimulation) was applied continuously to identify and preserve subcortical sites where interference occurred while the patient performed the HMt using a custom-made intraoperative piece of equipment requiring non-visually guided repetitive object manipulation with the contralesional hand (Figure 2A). The HMt is effective in mapping functional regions involved in complex hand movement, but also enables quantitative analysis of muscle activity, as the rhythmic movement produces a recurring EMG pattern[26,33] (Figure 2B). Interferences in EMG activity of hand and proximal upper limb muscles were concurrently on-line monitored by the neurophysiologist. The current intensity used was the same as was effective in producing HMt interferences during cortical mapping (mean intensity = 3.3mA, std = 0.9mA) when applied over the premotor cortex. If stimulation disrupted task execution during progression of the resection, the same site was verified by applying DES for two additional non-consecutive times. These sites were reported as ‘effective’. When subcortical stimulation produced a behavioural disturbance, this was reported by the neuropsychologist, and used as landmarks for establishing the functional boundaries of the resection and finally recorded using neuronavigation software (Curve, Brainlab AG, Munich, Germany). Task execution of each patient was videotaped for further offline analysis. To verify the LF-DES current threshold, i.e. the minimum intensity required to produce a task interference, each

effective site was re-assessed with DES by progressively decreasing the current in steps of 0.5mA[29]. Each effective site was also stimulated with high frequency DES (HF-DES) and the occurrence of motor evoked potentials (MEPs) in contralateral upper/lower limb and orofacial muscles was evaluated to estimate the distance from the corticospinal tract[35]. HF-DES was delivered using a constant current monopolar stimulator (straight tip, 1.5mm diameter, Inomed, with reference/ground on the skull overlying the central sulcus) in trains of 5 (To5) constant anodal current pulses (pulse duration: 5msec, interstimulus interval ISI: 3-4msec). Free-running EMG was recorded through all the procedure. Subdural electrocorticography (ECoG) of the precentral gyrus was recorded to detect DES-related afterdischarges or clinical seizures.

Offline EMG analysis

Each subcortical effective site identified during intraoperative HMt was inspected offline using the synchronised EMG recording and the videorecording of the behavioural execution. EMG-interference pattern associated to each effective site has been characterized by means of autocorrelation coefficient (aCC) and muscle recruitment analysis (RMS). Both parameters were calculated for abductor pollicis brevis (APB), extensor digitorum communis (EDC) and flexor dorsal interosseus (FDI), being the main intrinsic and extrinsic muscles involved in task execution.

A) aCC analysis was used to quantify the effect of DES on the regularity of phasic muscle contractions. The output results of aCC analysis for each muscle ranged from 0 (total loss of rhythmicity) to 1 (sustained rhythmicity). We then classified each effective site based on aCC average value among muscles in two EMG-interference patterns: *arrest pattern* (aCC = 0), reflecting a behavioural complete arrest of task execution (Video 1 and 2), or *clumsy pattern* (aCC > 0), referring to a spectrum of disruption of the phasic movement characterized by a progressive slowdown and/or loss of fingers coordination (Video 3 and 4).[26]

B) RMS analysis (Root Mean Square of the EMG signal) was used to quantify the effect of DES on motor unit recruitment. For each effective site and for each muscle, RMS was calculated and then normalized with respect to the RMS value of the same muscle during baseline movement (in absence of DES). Finally, for each effective site the RMS value was averaged among muscles. Effective sites were defined as 'negative' or 'positive' when RMS fell below or above the baseline respectively. Only negative effective sites were analysed in this study.

MR data

Data acquisition

All patients underwent MRI one day before surgery and at one-month follow-up. Preoperative MRI was performed on a Philips-Intera-3T scanner (Koninklijke Philips N.V. Amsterdam, Netherlands), and acquired for lesion morphological characterization and volumetric assessment. 15 patients underwent a HARDI-optimised diffusion imaging sequence using an eight-channel head coil. A spin echo, single shot EPI sequence was performed with 73 directions collected using a b-value of 2000s/mm3, and seven interleaved non-diffusion weighted (b0) volumes (TE:96ms, TR 10.4ms). The acquisition had a matrix size of 128x128 with an isotropic voxel size of 2mm3.

Extent of resection (EOR)

Extent of resection (volume resected with respect to tumour volume) was calculated on postoperative postcontrast MRI for enhancing lesions (target of resection) or FLAIR for nonenhancing lesions (target of resection) and classified on the basis of residual tumour volume (RTV) as total (RTV=0), subtotal (RTV $\leq$ 5mL), and partial (RTV>5mL). A supratotal resection was defined as the complete removal of any signal abnormalities, with the volume of the postoperative cavity larger than preoperative tumor volume.[31,36]

Registration of intraoperative stimulation sites

The spatial extent of the tested white matter area for each patient was evaluated during the intraoperative procedure on the preoperative T1/FLAIR used for neuronavigation and confirmed comparing the posterior border of the resection using the postoperative (1 month) MR image.

All effective sites were recorded by Brainlab software during the intraoperative procedure on the preoperative T1/FLAIR and confirmed extra-operatively using comparisons between the EMG and video-recordings of the resection and task execution. Resection cavities were delineated on the postoperative (1 month) MR image using ITK-SNAP, and both registered to a common template by means of lesion masking approach using the Clinical Toolbox in SPM (enantiomorphic normalization). Reliability of the normalisation process was visually inspected case-by-case. Sites were compared with the border of resection by the operating neurosurgeons (L.B.,M.R.). Details of the registration procedure are reported in the Supplementary Materials.

Probability density estimation of effective sites

The region of highest probability of producing a given EMG-interference pattern was calculated using probability density estimations[26] (PDE, see Supplementary Materials):
PDE for each hemisphere for arrest and clumsy pattern independently was computed. This map represents a 4D visualization of the anatomical region with the highest probability of inducing a given EMG-interference pattern, based on concentration of stimulation sites. A Dice coefficient of similarity, where 0 indicates no overlap and 1 indicates perfect overlap[37,38], was used to compare the overlap between the PDEs for arrest pattern and clumsy pattern within hemispheres, using the PDE thresholded between 15% and 85%.

Disconnectome analysis

To investigate white matter regions corresponding to different EMG-interference patterns, a disconnectome analysis was performed using each effective site as ROI. Following normalisation to MNI, a 6mm sphere was centred on the coordinates of each effective site in each patient. The sphere diameter was set in line with the proposed extent of stimulation of the bipolar probe.[39] Disconnectome maps were generated from the ROI spheres for each patient using BCBToolkit[25]. If an individual patient experienced the same effect at more than one site, both sites were used to generate the disconnectome map, however when more than one EMG-interference pattern was identified in different sites in the same patient, separate disconnectome maps were generated for each effect. The maps were generated from the tractography of 20 unrelated right-handed adults processed from the HCP 7T data release as part of BCB Toolkit (Supplementary table 1). This software tracks all white matter streamlines running through the responsive sites of each patient, to produce a percentage overlap map accounting for interindividual variability between the healthy control.[25] The disconnectome maps generate voxels showing the probability of disconnection from 0% to 100%. Each patient's disconnection profile was then used to investigate if specific white matter volumes would predict different EMG-interference patterns. To do so, nonparametric statistics were performed on disconnection maps thresholded at 90%, using FSL's *randomise* with 5000 permutations and threshold-free cluster enhancement (TFCE) to correct for multiple comparisons[40]. One sample t-tests were used with variance smoothing to assess which disconnection profiles were associated with the different EMG-interference pattern, in each hemisphere. The family-wise error threshold was set at $p < 0.05$. To identify the involved white matter tracts, we

superimposed the FSL-randomise outputs (contrast maps) with a white matter atlas computed on 1065 healthy subject[41] (WU-Minn HCP consortium data). For the specific purpose of the study, the HCP corticospinal projections were further dissected using the ROIs extracted from the Human Motor Template[42,43] in the following subcomponents: (i) primary motor cortex corticospinal tract (M1-CST); (ii) dorsal premotor cortex corticospinal tract (dPM-CST); (iii) ventral premotor cortex corticospinal tract (vPM-CST); (iv) supplementary motor area corticospinal tract (SMA-CST). We quantified the involved tracts based on the number of streamlines passing through the contrast maps out of the total amount of streamlines within the specific tracts. Results were expressed as a percentage of disconnected streamlines.

Diffusion tractography in individual patients

As the growth of brain tumours distorts anatomy, we tested and refined the disconnectome results in a subset of fifteen patients, comparing their stimulation sites (6mm-spherical ROIs) with their preoperative tractogram. Spherical deconvolution modelling and whole brain deterministic tractography was performed using StarTrack software. Virtual dissections of the white matter tracts highlighted by the previous analysis were performed by the first authors (H.H & L.V) using a region-of-interest (ROI) based approach, defining ROIs around regions of white matter reflecting the core of each tract. This included: projection fibres of (i) the primary motor cortex (M1-CST), (ii) the dorsal premotor cortex (dPM-CST), (iii) the ventral premotor cortex (vPM-CST) and (iv) the supplementary motor area (SMA-CST); striatal fibres of the superior frontal gyrus (Sup-FST) and of the inferior frontal gyrus (Inf-FST); association fibres including local u-shaped fibres connecting the middle frontal gyrus to the precentral gyrus (mid-U), the three branches of the superior-longitudinal fasciculus (SLFI, II and III), the frontal aslant tract (FAT) and the arcuate fasciculus (AF). This allows for visualisation of all fibres of a single tract without constraining its cortical projections, which may vary between subjects. Detailed description of the approach to tract dissection is described in previous studies.[15,24] Both the pre and postoperative T1 were registered to the spherical deconvolution anisotropic power diffusion map [44,45], for correct placement of the stimulation site on the tractogram.

Lesion symptom mapping and tract disconnection

In the post-operative phase (5 days from surgery), we assessed the presence of upper-limb motor impairment, using the MRC scale of muscle strength. To associate the postoperative

deficits with resected voxels we used a multivariate support vector regression lesion symptom mapping (SVR-LSM) using a Matlab toolbox released by DeMarco and Turkeltaub.[46] Two dependent variables were separately analysed: 1) the MRC score for motor deficits; 2) the De Renzi test score which assess the upper-limb ideomotor apraxia. During the test, patients were asked to imitate a variety (10 items) of intransitive gestures (not requiring the use of objects) with both the arm ipsilateral and that contralateral to the resection. No verbal description of the movements to be imitated was suggested. When an item was not reproduced correctly on the first demonstration, a second demonstration was given. Each item that was performed flawlessly on the first or second demonstration was scored 2 or 1, respectively; in case of unsatisfactory reproduction, the item was scored 0.[47] Only voxels resected in over 10% of patients were considered. Cluster-level family-wise error correction using permutation testing was applied (5000 permutations; statistical significance p=0.05). As resection volume can be a confounding factor in voxel-behaviour correlations, we controlled for this using a direct total lesion volume control (DTLVC)[48]. The significant cluster was compared with the AAL atlas[49] and an atlas of white matter.[41] In patients with tractography, the resection cavities were used as exclusion ROIs within TrackVis software to calculate the percentage of streamlines remaining for each tract.

Data Availability Statement

The data that support the findings of this study is available from the corresponding author, upon reasonable request. The metadata generated in this study is available through Mendeley Data at the following address: doi: 10.17632/xpbct2hw2v.1.

Results

Anatomical and demographic characteristics

Table 1. Demographic and clinical information on the entire sample.

Thirty-four patients were included in the study. Patient demographics are summarized in Table 1 (mean age 42 years, s.d. 10.6; 17 male, 4 left-handers). In 23 patients a supratotal resection and in 11 a total resection was performed.

Anatomically segregated effects of DES on hand muscles

Although the right frontal white matter was explored more than the left due to functional (language) constraints, a common area tested in both hemispheres was clearly detected and involved the deep white matter above (3cm) the central sulcus (Figure 2C). Within the stimulated area, the arrest pattern (aCC=0) was found in 36 sites (54%; 27 in right and 9 in left hemisphere), while the clumsy pattern (aCC>0) was found in 30 sites (46%, 15 in right and 15 in left hemisphere) (Figure 3A, B, C). In 11 patients, both type patterns were observed at different sites. Although muscle suppression occurred in both patterns, when arrest occurred the suppression was significantly higher and affected all muscles (Mann-Whitney U-test, u=178, p=<0.0001). The distribution of aCC and RMS values for each effective site is reported in Supplementary Materials. Notably, when reducing the current intensity below threshold by 0.5mA, LF-DES stimulation of each eloquent site failed in evoking any task interference both at behavioral and EMG level showing that the features of the EMG-patterns were not changing according to the intensity of current used.

When effective sites were stimulated with HF-DES (To5) up to 10 mA of intensity, no upper-limb MEPs were never elicited, suggesting a distance of at least 10mm to the M1-CST[35,50–53]. An additional analysis showing the distance between the stimulation sites and the trajectory of the M1-CST is reported in Supplementary Materials.

Anatomical localisation of the arrest and clumsy patterns were computed by means of probability density estimation in each hemisphere. The two patterns were partially overlapped mainly below the middle frontal gyrus (right hemisphere Dice coefficient=0.42, left hemisphere Dice coefficient=0.09). However, the two patterns showed a preferential dorso-ventral distribution: 1) the arrest pattern occurred bilaterally in the white matter below the dorsal premotor region (Figure 3B-D); 2) the clumsy pattern occurred bilaterally in the white matter below the ventral premotor region, and, only in the left hemisphere, 4 sites out of 15 were reported in the middle anterior cingulum below the pre-SMA (Figure 3C-E). This distribution was confirmed also in the 11 patients in which both patterns were recorded.

Structural connections linked to different EMG-interference patterns

Disconnectome results

Disconnectome probability maps were created for each patient. Non-parametric one-sample t tests were run across patients to identify the white matter connections associated with the arrest

or the clumsy pattern. Regression showed a dorso-ventral distribution reflecting the results of the probability density estimation (Figure 3D, E) (see previous section): in both hemispheres, the arrest pattern was associated with the disconnection of dorsal-mesial white matter, while the clumsy pattern with ventral white matter (TFCE, p-fwer <0.05) (Figure 4A, B). After comparison with a white matter atlas[41], we quantified the percentage of disconnected streamlines for each tract possibly running through this region (Figure 4C-H, supplementary table 2). The tracts most often recruited included association fibres: short U-shaped precentral tracts (mid-U-shaped), the superior longitudinal fasciculus (SLF I, II and III branches), the frontal aslant tract (FAT), the arcuate fasciculus (AF); projection fibres: the superior and inferior frontostriatal tracts (SupFST, InfFST), projections between the cerebral peduncle and (i) the primary motor cortex (M1-CST), (ii) the dorsal premotor cortex (dPM-CST), (iii) the ventral premotor cortex (vPM-CST) and (iv) the supplementary motor area (SMA-CST); and callosal fibres (although these were not further analysed). Short range premotor mid-U-shaped fibres were exclusively associated with the arrest pattern, while inferior fronto-striatal fibres and the superior longitudinal fasciculus III were uniquely associated with the clumsy pattern. Despite the significant structural segregation, a set of common pathways were associated to both effects, including the superior fronto-striatal tract, corticospinal projections, the frontal aslant tract, the arcuate and the superior longitudinal fascisulus I and II.

Individual patients tractography results

The tracts identified with the disconnectome analysis were reconstructed by tractography in a subset of fifteen patients (Table 2; 7 left hemisphere; 8 right hemisphere). In these patients, 27 sites were identified: in 15 sites (4 left hemisphere, 11 right) DES induced arrest pattern, in 12 (5 left hemisphere, 7 right) a clumsy pattern. The location of each site was crossed by dissected tracts in all cases, except for M1-CST and vPM-CST.

Table 2. Tract measurements for the 15 patients with diffusion tractography

Considering white matter variability due to individual differences and possible tract dislocation due to tumour growth, the dissection of tracts at the individual subject level and correlation with stimulation sites improved the reliability and specificity of results. Results clearly showed that stimulation affected tracts running in the frontal white matter below dorsal premotor, producing the arrest pattern, and that stimulation of tracts in the frontal white matter below

ventral premotor produced the clumsy pattern. This confirmed the results of disconnectome analysis and reduced the amount of overlap between effects. To improve the sampling, results were grouped irrespective of hemisphere. Figure 5A shows the frequencies of the two EMG-interference patterns within the studied tracts and 5B shows the number of stimulations for each tract and pattern. We considered a single tract to be linked to a specific EMG-interference pattern when the latter was evoked by more than 80% of stimulation occurrences with the given tract. Tracts associated with the arrest pattern were the mid-U-shaped fibres, the superior longitudinal fasciculus II (10 out 11 stimulations), the superior fronto-striatal tract (9 out 11 stimulations), the dPM-CST fibres (5 stimulation out of 6), the SMA-CST fibres (7 out of 8 stimulations) and the superior longitudinal fasciculus I (6 out of 6 stimulations) (Figure 5C). The clumsy pattern was associated with the superior longitudinal fasciculus III and the arcuate fasciculus (8 out 8 stimulations) and with the inferior fronto-striatal tract (7 out of 7 stimulations) (Figure 5D). The frontal aslant tract was linked to both arrest pattern (5 out of 13 stimulations) and clumsy pattern (8 out of 13 stimulations) (Figure 5E). No effective site was located within the trajectory of the M1-CST and vPM-CST. Figure 5 (F-J) shows a patient with multiple stimulation sites and their relationship with white matter tracts.

Resection of dorsal white matter was associated to transient post-operative upper-limb motor deficit

Eleven patients out of 34 experienced transient postoperative MRC deficits at 5 days from surgery, completely recovered at the one-month follow up (Table 1). Figure 6A reports the common resected area in all patients. SVR-LSM showed the association of the MRC deficit with a cluster of voxels located in the white matter below the right superior frontal gyrus, including the SMA, mesial to the mid-anterior cingulate cortex (mACC) ($p=0.05$; 5000 permutations, Figure 6B). In the left hemisphere only three patients experienced post-operative MRC deficits, thus no significant voxels emerged. The significant cluster overlapped only with the arrest pattern density map (134 voxels in common) and corresponded with the dorsal white matter region enclosing mainly SMA-projections and the superior fronto-striatal tracts (Figure 6C, D). No overlap emerged with the region where DES elicited the clumsy pattern. Finally, we evaluated the impact of resection on the eleven investigated tracts in the fifteen patients with tractography. In this group, only three patients experienced transient MRC deficits. In all of this group over 50% of resection cavities enclosed the dorsal frontal white matter region,

including mid-U-shaped fibres, SMA-CST and superior fronto-striatal fibres. Notably, in all fifteen patients, the frontal aslant tract, the three branches of the superior longitudinal fasciculus, the arcuate and the inferior fronto-striatal tract were commonly resected without any association with MRC upper-limb deficit or apraxia (Figure 6E). M1-CST and vPM-CST were never resected in any patient. In addition to MRC evaluation, we also performed a SVR-LSM for upper-limb ideomotor apraxia. We excluded the patients with postoperative MRC deficits from this analysis. In both hemispheres no significant clusters emerged. Only one patient had a pathological score in the De Renzi test in the immediate postoperative phase (Table 1), which fully recovered at the one-month follow-up. This observation is consistent with previous findings showing that surgery guided by intraoperative HMt reduces immediate and long-term post-operative praxis deficits[33].

Discussion

In this study we aimed at identifying the frontal lobe connections involved in hand-muscle control during the performance of an ecologically relevant hand-object manipulation task, by using subcortical DES during the awake phase of neurosurgical procedures of 34 patients. Results of the intraoperative brain mapping, EMG-interference pattern analysis and diffusion tractography point to the existence of two different white matter regions associated to distinct aspect of task-related motor output implementation. We evaluated the effect of permanent disconnection of different white matter tracts on immediate post-operative motor outcome using two commonly used clinical tests, the MRC scale of muscle strength and the De Renzi test for ideomotor apraxia. The preservation during surgery of dorsal white matter surrounding the supplementary motor area is crucial to preserve upper-limb movement integrity in the immediate post-operative phase, although in the ventral region no motor deficit was detected with these clinical tests.

Probability density estimation of EMG-interference patterns

DES evoked either complete disruption of hand-muscle activity required for task execution (arrest pattern), or a partial disruption consisting of a spectrum of milder effects ranging from movement slowdown to a loss of finger coordination (clumsy pattern). Localisation based on probability density estimation (PDE) of the two interference patterns showed that, although they overlapped below the middle frontal gyrus, the arrest pattern occurred preferentially during stimulation of white matter below a dorsal premotor region anterior to the precentral

hand-knob, whereas the clumsy pattern occurred preferentially within white matter below ventral premotor region. In a previous study adopting the same methodological approach to investigate cortical premotor areas similar EMG-interference patterns were identified on the precentral convexity[24]. The arrest pattern was reported in both ventral (vPM) and dorsal (dPM) premotor cortex, although in the latter it was associated with mixed suppression-recruitment effects (an initial period of muscle suppression followed by a progressive recruitment of motor units). The clumsy pattern was instead reported exclusively in vPM, with different degrees of muscle suppression. The homologies and differences emerging along the dorso-ventral direction with the present study might be due to differences in the neural elements stimulated with DES (cortical vs subcortical). Stimulation can evoke inhibitory or excitatory effects within local neuronal populations depending on its proximity to grey or white matter.[54] Despite local and remote neurophysiological effects induced by DES are still poorly understood, in line with the previous study[26], we suggest that the two EMG-interference patterns may result from stimulation of different neuronal substrates: the arrest pattern may reflect the disruption of a network closely involved in motor output implementation, while the clumsy pattern may reflect the perturbation of a network possibly involved in sensorimotor computations required for task execution.

Disconnectome and tractography in single patients

To predict which white matter connections were associated to the different EMG-interference patterns, we used a disconnectome analysis[25], assuming that DES caused a transient disconnection of the workflow information between interconnected structures. The arrest and clumsy patterns were associated respectively with disconnection of different dorsal and ventral white matter pathways, in line with the results shown by PDE. Within these regions, we identified specific and common white matter tracts for the two interference patterns. Short range premotor mid-U-shaped fibres were only associated with the arrest pattern, while inferior fronto-striatal fibres and the superior longitudinal fasciculus III were uniquely associated with the clumsy pattern. Despite the significant structural segregation, both effects could result from the interference of the activity of corticospinal fibres from primary and premotor areas. Permanent disconnection of these fibres has been extensively correlated to deficits in dexterity[55–57]. Moreover, a set of common striatal and associative pathways, including the superior fronto-striatal tract, the frontal aslant tract, the arcuate and the superior longitudinal fascisulus I and II, were correlated to both effects.

To improve the specificity of the atlas-based disconnectome results, we used preoperative tractography in fifteen patients to assess the disconnected tracts based on their own stimulation sites. This analysis refined the previous results to show that: 1) transient disconnection of dorsal white matter including local mid-U-shaped fibres together with the superior longitudinal fasciculus I and II, the superior fronto-striatal tract and corticospinal projections of dPM and SMA was preferentially associated with the arrest pattern; 2) transient disconnection of ventral white matter, including the inferior fronto-striatal tract, the superior longitudinal fasciculus III and the arcuate instead produced the clumsy pattern; 3) precentral corticospinal fibres (linked to M1and vPM) were not affected by stimulation, as no sites were in the vicinity of these connections. The dorsal region, differently from the ventral one, has direct access to the spinal cord via SMA/dPM-CST and both direct/indirect connections with primary motor output via basal ganglia-thalamo-cortical loops and local motor-premotor U-shaped fibres. This result agrees with the hypothesis that the arrest pattern may reflect the perturbation of a network hierarchically proximal to the motor output. Coherently, lesion analysis showed that resection of the dorsal white matter region (i.e., mid-U fibres, SMA projections and Sup-FST), but not of the ventral one, was significantly associated with short-term MRC post-operative upper limb deficit.

Arrest of movement occurs stimulating white matter below dorsal premotor area

The arrest pattern occurred when DES was applied below dorsal premotor cortex where cortico-fugal, cortico-striatal, and cortico-cortical projections intersect. Although this study does not provide conclusive evidence whether the effect induced by DES results from the stimulation of one or multiple white matter pathways, non-human primate studies may suggest some interpretations.

Since no muscle contractions were elicited when stimulating the hand at rest within this region, nor even when stimulating with high frequency DES and progressively increasing current intensity (until 10mA, an intensity corresponding approximately to a distance of 10mm to the CST[35,50–53]), we reasonably ruled out the involvement of the corticospinal tract originating from the primary motor area. However, as also highlighted by tractography results, projections descending from the dPM and the SMA should be considered. In non-human primates, the SMA and dPM have direct access to the spinal cord, with dense terminations to inhibitory

interneurons of the intermediate zone, mainly in lateral lamina VII.[58,59] Coherently, DES applied in a region dense with cortico-fugal fibres may have caused abnormal activation of inhibitory spinal circuits leading to the muscle suppression observed in the task arrest pattern. In accordance with this hypothesis, optogenetic stimulation of spinal inhibitory interneurons arrests the voluntary motor output.[60]

Inhibition of ongoing upper limb movement occurs in non-human primates during stimulation of white matter superior to the dorsal striatum[61,62]. Direct and indirect cortico-thalamic loops via the basal ganglia guarantee motor inhibition, a key component of adaptive behaviour.[3,63,64] In our cohort of patients, stimulation of superior fronto-striatal fibres may have altered the excitatory-inhibitory balance within the basal ganglia circuits, eventually affecting the excitability of the primary motor output. In humans, this hypothesis is coherent with previous intraoperative studies suggesting that the arrest of repetitive flexion-extension of the arm might be induced by stimulation of cortico-striatal tracts.[65,66]

Short association U-shaped fibres connecting the hand-knob sector of primary motor cortex with the middle frontal gyrus may also have been implicated in facilitating hand-object interaction. In a previous study, using the same task[28], DES of the anterior hand-knob region hosting caudal U-shaped terminations evoked task arrest concomitant to suppression of hand muscles. This preliminary result suggests that these fibres may play an inhibitory role on the primary motor output, an-hypothesis supported by non-human primate data reporting a short-latency powerful inhibition of M1 output due to a conditioning stimulation of dPM area.[67] Premotor short association tracts have been identified in humans using postmortem methods[68], diffusion tractography[69,70] and 7T MRI[71] and have been theorised to be the human homologues of the cortico-cortical premotor connections engaged in the monkey reaching and grasping system.[69,72]

The dorsal white matter area is also a region crossed by fronto-parietal connections recognised to be responsible for different processes of sensorimotor integrations required by hand action in non-human primates[11]. The dorsal branch of the superior longitudinal fasciculus (SLF I) has been linked to manual specialization and lateralised hand selection[24,73], while the middle branch (SLFII) seems to be involved in higher order sensorimotor transformation for reaching and grasping and oculomotor exploration.[23,24,74,75] Possibly, the SLFI/II, in addition to its visuomotor functions, may also transmit relevant proprioceptive and tactile information required for controlling finger coordination during haptically guided object manipulation. However, considering the functional aspects associated with these pathways and that the HMt

is performed in absence of visual guidance, it seems not reasonable to hypothesize that DES of the SLFI/II could evoke a massive distal muscle suppression.

Finally, DES may have also perturbed the excitability of the contralateral motor areas via transcallosal fibres connecting the contralateral motor-premotor areas. In this regard, it has been shown that interhemispheric inhibition is a key component in fine dextrous motor control, mediated via motor transcallosal fibres[76–78].

Clumsy movement occurs when stimulating white matter below ventral premotor area

The clumsy pattern was characterised by a low level of regularity between phasic muscle contractions and behaviourally shows a progressive movement slowdown and loss of finger coordination. It occurred with highest probability in a white matter region below the ventral premotor area, mainly occupied by fronto-parietal and inferior fronto-striatal connections.

This region contains fibres of the superior longitudinal fasciculus III, connecting the supramarginal gyrus (anterior inferior parietal lobule) with inferior frontal regions.[79] The disconnectome analysis indicated this fascicle may be affected by stimulation in the right hemisphere only. However, this result may have been influenced by the strong right-ward asymmetry of this tract described in literature[23,24,80]. In fact, when examining the patients with tractography, we showed that in fact stimulation had affected the SLFIII in both hemispheres. Anatomo-functional studies in non-human primates report this connection as the most likely homologue of the AIP/PFG-F5 circuit underlying grasp-related sensorimotor transformations in macaques[5]. In the non-human primate, the PFG/AIP connections with the anterior premotor area F5 represent the core of a large-scale network for purposeful hand action, integrating sensorimotor and cognitive information[74]. Interestingly, using behavioural inspection, the clumsy pattern resembled symptoms associated with myelo/limb-kinetic apraxia.[81] Patients with this disorder cannot accurately realize fine motor acts, such as turning a key into a lock. Limb-kinetic apraxia occurs in frontal lesions and its nature is controversial, as it is difficult to disentangle this higher order deficit from a concurrent limb weakness.[82] Fogassi and colleagues[83] also highlighted the similarity between this condition and impairment in hand-shaping after reversible inactivation of monkey vPM during visually guided grasping in macaques. A similar pattern of interference has been reported in humans when vPM is virtually

lesioned by transcranial magnetic stimulation during a precision grip task, which affects accurate finger adjustments on the object.[84] Notably, the superior longitudinal fasciculus III has cortical terminations in the dorsal sector of vPM, where DES during the HMt evoked the same clumsy pattern.[26] Moreover, information coming from the human right and left inferior parietal lobe seem crucial in perception of our own limbs and in somatic perception of hand-object interactive movement respectively[85,86]. Overall, the effects evoked by DES-related transient disconnection of the superior longitudinal fasciculus III during HMt might reflect disruption of information carried between the parietal and premotor cortex.

Disconnectome and tractography results also showed that the clumsy pattern may have been induced by stimulation of inferior fronto-striatal fibres. Again, this data is coherent with the anatomo-functional organisation of the macaque lateral grasping network, where ventral premotor send inputs to specific sectors of the putamen.[87] Notably the limb-kinetic apraxia is a symptom of neurodegenerative disorders involving the basal ganglia, such as progressive supranuclear palsy and Parkinson disease. In this view, the apraxic symptoms, and the clumsy pattern observed in the present study, may reflect combined cortico-cortical connections to ventral premotor area and cortico-striatal dysfunction.[82]

The frontal aslant tract

Finally, the association of the frontal aslant tract with both the arrest and clumsy pattern deserves discussion. The FAT is an intra-lobar tract connecting the SMA/preSMA region with the posterior inferior frontal gyrus[69], which intersects both the dorsal and ventral regions emerging in our analysis. The double effect associated with the frontal aslant tract may be due to its stimulation at the intersection with the tracts actually mediating the effect, challenging its direct involvement. Alternatively, we speculate that DES delivered along the FAT may affect task execution by acting indirectly on the ventral and dorsal node, possibly via their common cortical sources. The functional role of the FAT is diverse, being associated with speech and language[88], working memory[89] and visually guided upper-limb movements[90]. However, the lesion analysis here showed this pathway could be resected without postoperative motor deficit, which may suggest it plays an indirect role in motor output control.

Association between permanent disconnection and motor outcome

Results showed that partial resection of the SMA and surrounding white matter was associated with an immediate postoperative upper-limb motor impairment, fully recovered at the one-month follow-up. This result is coherent with the transient akinesia or 'SMA syndrome' described in the neurosurgical literature after SMA resection[91] and with human studies predicting motor outcome after stroke based on dorsal premotor white matter integrity.[92,93] This result was confirmed in a subset of patients with preoperative diffusion tractography. In this cohort, the absence of motor deficit occurred only when SMA-projections and mid-U-shaped connections to M1 were spared. This supports our hypothesis, suggesting a functional proximity of the dorsal white matter region to the hand-related motor output. Overall, our results highlighted the clinical importance of preserving SMA fibres, whose correlation with motor deficit was demonstrated in patients with subcortical stroke[55]. On the other hand, the frontal aslant tract, the arcuate, the three branches of the superior longitudinal fasciculus and the inferior fronto-striatal fibres were commonly resected without any motor disturbances. Resection of the latter tracts might rather be associated to higher sensorimotor disorders, such as ideomotor apraxia. However, SVR-LSM for this clinical variable did not show, in the sample of patients analysed, any significant clusters, leaving this issue unsolved.

Limitations

The intraoperative setting, while providing a unique opportunity for studying the role of tracts, has some intrinsic limitations. The area to be stimulated in single patients cannot be established *a priori* for research purposes, but entirely depends on the surgical strategy. For this reason, the left hemisphere was less investigated in terms of the number of stimulation sites, as language tests were also performed to assess the posterior border of the resection. It is also not possible to study subtle hemispheric differences using DES, as patients cannot be tested in both hemispheres. As tumour location and surgical strategy establish the area available for testing with stimulation, it would be important to confirm these results in an even higher number of patients with diffusion tractography and taking advantage of advanced electrophysiological recording techniques[94]. Finally, our intraoperative task was haptically performed, in order to focus mainly on the motor domain of hand-object manipulation, thus results cannot be attributed to mechanisms underlying visual guidance and/or reaching phase of the movement.

Acknowledgements

We are very grateful to Roger Lemon and Stephanie Forkel for their helpful comments on the manuscript. Data were provided in part from the HCP, WU-Minn Consortium (Principal Investigators: David Van Essen and Kamil Ugurbil; 1U54MH091657) funded by the 16 NIH Institutes and Centers that support the NIH Blueprint for Neuroscience Research; and by the McDonnell Center for Systems Neuroscience at Washington University in St. Louis.

Funding

This work has been supported by "Regione Lombardia" under the Eloquentstim Project (PorFesr, 2014–2020) to G.C. and by a grant from Associazione Italiana per la Ricerca sul Cancro (AIRC) to L.B.

Competing interests

The authors have no conflicting interests to report.

Supplementary material

Supplementary material is available at *Brain* online.

References

1. Almécija S, Smaers JB, Jungers WL. The evolution of human and ape hand proportions. *Nat Commun*. 2015;6(1):1-11. doi:10.1038/ncomms8717
2. Lemon RN. Descending pathways in motor control. *Annu Rev Neurosci*. 2008;31:195-218. doi:10.1146/annurev.neuro.31.060407.125547
3. Alexander GE, Crutcher MD. Functional architecture of basal ganglia circuits: neural substrates of parallel processing. *Trends Neurosci*. 1990;13(7):266-271. doi:10.1016/0166-2236(90)90107-L
4. Aron AR, Durston S, Eagle DM, Logan GD, Stinear CM, Stuphorn V. Converging evidence for a fronto-basal-ganglia network for inhibitory control of action and cognition. In: *Journal of Neuroscience*. Vol 27. Society for Neuroscience; 2007:11860-11864. doi:10.1523/JNEUROSCI.3644-07.2007
5. Borra E, Gerbella M, Rozzi S, Luppino G. The macaque lateral grasping network: A neural substrate for generating purposeful hand actions. *Neurosci Biobehav Rev*. 2017;75:65-90. doi:10.1016/j.neubiorev.2017.01.017
6. Cisek P, Kalaska JF. Neural mechanisms for interacting with a world full of action choices. *Annu Rev Neurosci*. 2010;33:269-298. doi:10.1146/annurev.neuro.051508.135409
7. Ebbesen CL, Brecht M. Motor cortex - To act or not to act? *Nat Rev Neurosci*. 2017;18(11):694-705. doi:10.1038/nrn.2017.119
8. Gallivan JP, Chapman CS, Wolpert DM, Flanagan JR. Decision-making in

sensorimotor control. *Nat Rev Neurosci*. 2018;19(9):519-534. doi:10.1038/s41583-018-0045-9
9. Thiebaut de Schotten M, Foulon C, Nachev P. Brain disconnections link structural connectivity with function and behaviour. *Nat Commun*. 2020;11(1):1-8. doi:10.1038/s41467-020-18920-9
10. Gharbawie OA, Stepniewska I, Qi H, Kaas JH. Multiple parietal-frontal pathways mediate grasping in macaque monkeys. *J Neurosci*. 2011;31(32):11660-11677. doi:10.1523/JNEUROSCI.1777-11.2011
11. Battaglia-Mayer A, Caminiti R. Corticocortical systems underlying high-order motor control. *J Neurosci*. 2019;39(23):4404-4421. doi:10.1523/JNEUROSCI.2094-18.2019
12. Howells H, Simone L, Borra E, Fornia L, Cerri G, Luppino G. Reproducing macaque lateral grasping and oculomotor networks using resting state functional connectivity and diffusion tractography. *Brain Struct Funct*. 2020;225(8):2533-2551. doi:10.1007/s00429-020-02142-2
13. Graziano MSA, Aflalo TN. Mapping behavioral repertoire onto the cortex. *Neuron*. 2007;56(2):239-251. doi:10.1016/j.neuron.2007.09.013
14. Fornia L, Puglisi G, Leonetti A, et al. Direct electrical stimulation of the premotor cortex shuts down awareness of voluntary actions. *Nat Commun*. 2020;11(1):1-11. doi:10.1038/s41467-020-14517-4
15. Catani M, Thiebaut de Schotten M. *Atlas of Human Brain Connections*. Oxford University Press; 2012. doi:10.1093/med/9780199541164.001.0001
16. Barrett RLC, Dawson M, Dyrby TB, et al. Differences in frontal network anatomy across primate species. *J Neurosci*. 2020;40(10):2094-2107. doi:10.1523/JNEUROSCI.1650-18.2019
17. Coscia M, Wessel MJ, Chaudary U, et al. Neurotechnology-aided interventions for upper limb motor rehabilitation in severe chronic stroke. *Brain*. 2019;142(8):2182-2197. doi:10.1093/brain/awz181
18. Micera S, Caleo M, Chisari C, Hummel FC, Pedrocchi A. Review Advanced Neurotechnologies for the Restoration of Motor Function. *Neuron*. 2020;105:604-620. doi:10.1016/j.neuron.2020.01.039
19. Bello L, Riva M, Fava E, et al. Tailoring neurophysiological strategies with clinical context enhances resection and safety and expands indications in gliomas involving motor pathways. *Neuro Oncol*. 2014;16(8):1110-1128. doi:10.1093/neuonc/not327
20. Duffau H. Stimulation mapping of white matter tracts to study brain functional connectivity. *Nat Rev Neurol*. 2015;11(5):255-265. doi:10.1038/nrneurol.2015.51
21. Puglisi G, Howells H, Leonetti A, et al. Frontal pathways in cognitive control: direct evidence from intraoperative stimulation and diffusion tractography. *Brain*. 2019;142(8):2451-2465. doi:10.1093/brain/awz178
22. Moving Beyond DTI. In: *Introduction to Diffusion Tensor Imaging*. Elsevier; 2014:65-78. doi:10.1016/b978-0-12-398398-5.00008-4
23. Budisavljevic S, Dell'Acqua F, Zanatto D, et al. Asymmetry and Structure of the Fronto-Parietal Networks Underlie Visuomotor Processing in Humans. *Cereb Cortex*. 2017;27(2):1532-1544. doi:10.1093/cercor/bhv348
24. Howells H, De Schotten MT, Dell'Acqua F, et al. Frontoparietal tracts linked to lateralized hand preference and manual specialization. *Cereb Cortex*. 2018;28(7). doi:10.1093/cercor/bhy040
25. Foulon C, Cerliani L, Kinkingnéhun S, et al. Advanced lesion symptom mapping analyses and implementation as BCBtoolkit. *Gigascience*. 2018;7(3):1-17. doi:10.1093/gigascience/giy004
26. Fornia L, Rossi M, Rabuffetti M, et al. Direct electrical stimulation of premotor areas:

Different effects on hand muscle activity during object manipulation. *Cereb Cortex*. 2020;30(1):391-405. doi:10.1093/cercor/bhz139
27. Simone L, Fornia L, Viganò L, et al. Large scale networks for human hand-object interaction: Functionally distinct roles for two premotor regions identified intraoperatively. *Neuroimage*. 2020;204:116215. doi:10.1016/j.neuroimage.2019.116215
28. Viganò L, Fornia L, Rossi M, et al. Anatomo-functional characterisation of the human "hand-knob": A direct electrophysiological study. *Cortex*. 2019;113:239-254. doi:10.1016/j.cortex.2018.12.011
29. Viganò L, Howells H, Fornia L, et al. Negative motor responses to direct electrical stimulation: Behavioral assessment hides different effects on muscles. *Cortex*. 2021;137:194-204. doi:10.1016/j.cortex.2021.01.005
30. Leonetti A, Puglisi G, Rossi M, et al. Factors Influencing Mood Disorders and Health Related Quality of Life in Adults With Glioma: A Longitudinal Study. *Front Oncol*. 2021;11:1. doi:10.3389/fonc.2021.662039
31. Rossi M, Gay L, Ambrogi F, et al. Association of Supratotal Resection with Progression-Free Survival, Malignant Transformation, and Overall Survival in Lower-Grade Gliomas. *Neuro Oncol*. Published online October 13, 2020. doi:10.1093/neuonc/noaa225
32. Rossi M, Nibali MC, Viganò L, et al. Resection of tumors within the primary motor cortex using high-frequency stimulation: oncological and functional efficiency of this versatile approach based on clinical conditions. *J Neurosurg*. 2020;133(3):642-654. doi:10.3171/2019.5.JNS19453
33. Rossi M, Fornia L, Puglisi G, et al. Assessment of the praxis circuit in glioma surgery to reduce the incidence of postoperative and long-term apraxia: a new intraoperative test. *J Neurosurg*. 2018;130(1):17-27. doi:10.3171/2017.7.JNS17357
34. Conti Nibali M, Leonetti A, Puglisi G, et al. Preserving Visual Functions During Gliomas Resection: Feasibility and Efficacy of a Novel Intraoperative Task for Awake Brain Surgery. *Front Oncol*. 2020;10:1485. doi:10.3389/fonc.2020.01485
35. Raabe A, Beck J, Schucht P, Seidel K. Continuous dynamic mapping of the corticospinal tract during surgery of motor eloquent brain tumors: evaluation of a new method. *J Neurosurg*. 2014;120(5):1015-1024. doi:10.3171/2014.1.JNS13909
36. Rossi M, Ambrogi F, Gay L, et al. Is supratotal resection achievable in low-grade gliomas? Feasibility, putative factors, safety, and functional outcome. *J Neurosurg*. Published online May 17, 2019:1-14. doi:10.3171/2019.2.JNS183408
37. Dice LR. Measures of the Amount of Ecologic Association Between Species. *Ecology*. 1945;26(3):297-302. doi:10.2307/1932409
38. Zou KH, Warfield SK, Bharatha A, et al. Statistical Validation of Image Segmentation Quality Based on a Spatial Overlap Index. *Acad Radiol*. 2004;11(2):178-189. doi:10.1016/S1076-6332(03)00671-8
39. Haglund MM, Ojemann GA, Blasdel GG. Optical imaging of bipolar cortical stimulation. *J Neurosurg*. 1993;78(5):785-793. doi:10.3171/jns.1993.78.5.0785
40. Winkler AM, Ridgway GR, Webster MA, Smith SM, Nichols TE. Permutation inference for the general linear model. *Neuroimage*. 2014;92:381-397. doi:10.1016/j.neuroimage.2014.01.060
41. Yeh FC, Panesar S, Fernandes D, et al. Population-averaged atlas of the macroscale human structural connectome and its network topology. *Neuroimage*. 2018;178:57-68. doi:10.1016/j.neuroimage.2018.05.027
42. Mayka MA, Corcos DM, Leurgans SE, Vaillancourt DE. Three-dimensional locations and boundaries of motor and premotor cortices as defined by functional brain imaging:

A meta-analysis. *Neuroimage*. 2006;31(4):1453-1474. doi:10.1016/J.NEUROIMAGE.2006.02.004
43. Archer DB, Vaillancourt DE, Coombes SA. A Template and Probabilistic Atlas of the Human Sensorimotor Tracts using Diffusion MRI. *Cereb Cortex*. 2018;28(5):1685-1699. doi:10.1093/CERCOR/BHX066
44. Chen DQ, Dell'Acqua F, Rokem A, et al. Diffusion Weighted Image Co-registration: Investigation of Best Practices. *bioRxiv*. Published online December 2019:864108. doi:10.1101/864108
45. Dell'Acqua F, Simmons A, Williams SCR, Catani M. Can spherical deconvolution provide more information than fiber orientations? Hindrance modulated orientational anisotropy, a true-tract specific index to characterize white matter diffusion. *Hum Brain Mapp*. 2013;34(10):2464-2483. doi:10.1002/hbm.22080
46. DeMarco AT, Turkeltaub PE. A multivariate lesion symptom mapping toolbox and examination of lesion-volume biases and correction methods in lesion-symptom mapping. *Hum Brain Mapp*. 2018;39(11):4169-4182. doi:10.1002/hbm.24289
47. De Renzi E, Motti F, Nichelli P. Imitating Gestures: A Quantitative Approach to Ideomotor Apraxia. *Arch Neurol*. 1980;37(1):6-10. doi:10.1001/archneur.1980.00500500036003
48. Zhang Y, Kimberg DY, Coslett HB, Schwartz MF, Wang Z. Multivariate lesion-symptom mapping using support vector regression. *Hum Brain Mapp*. 2014;35(12):5861-5876. doi:10.1002/hbm.22590
49. Tzourio-Mazoyer N, Landeau B, Papathanassiou D, et al. Automated anatomical labeling of activations in SPM using a macroscopic anatomical parcellation of the MNI MRI single-subject brain. *Neuroimage*. 2002;15(1):273-289. doi:10.1006/nimg.2001.0978
50. Kamada K, Todo T, Ota T, et al. The motor-evoked potential threshold evaluated by tractography and electrical stimulation: Clinical article. *J Neurosurg*. 2009;111(4):785-795. doi:10.3171/2008.9.JNS08414
51. Nossek E, Korn A, Shahar T, et al. Intraoperative mapping and monitoring of the corticospinal tracts with neurophysiological assessment and 3-dimensional ultrasonography-based navigation. Clinical article. *J Neurosurg*. 2011;114(3):738-746. doi:10.3171/2010.8.JNS10639
52. Ohue S, Kohno S, Inoue A, et al. Accuracy of Diffusion Tensor Magnetic Resonance Imaging-Based Tractography for Surgery of Gliomas Near the Pyramidal TractA Significant Correlation Between Subcortical Electrical Stimulation and Postoperative Tractography. *Neurosurgery*. 2012;70(2):283-294. doi:10.1227/NEU.0B013E31823020E6
53. Prabhu SS, Gasco J, Tummala S, Weinberg JS, Rao G. Intraoperative magnetic resonance imaging–guided tractography with integrated monopolar subcortical functional mapping for resection of brain tumors: Clinical article. *J Neurosurg*. 2011;114(3):719-726. doi:10.3171/2010.9.JNS10481
54. Mohan UR, Watrous AJ, Miller JF, et al. The effects of direct brain stimulation in humans depend on frequency, amplitude, and white-matter proximity. *Brain Stimul*. 2020;13(5):1183-1195. doi:10.1016/j.brs.2020.05.009
55. Liu J, Wang C, Qin W, et al. Corticospinal Fibers With Different Origins Impact Motor Outcome and Brain After Subcortical Stroke. *Stroke*. 2020;51:2170-2178. doi:10.1161/STROKEAHA.120.029508
56. Newton JM, Ward NS, Parker GJM, et al. Non-invasive mapping of corticofugal fibres from multiple motor areas—relevance to stroke recovery. *Brain*. 2006;129(0 7):1844. doi:10.1093/BRAIN/AWL106

57. Potter-Baker KA, Varnerin NM, Cunningham DA, et al. Influence of Corticospinal Tracts from Higher Order Motor Cortices on Recruitment Curve Properties in Stroke. *Front Neurosci*. 2016;0(MAR):79. doi:10.3389/FNINS.2016.00079
58. McNeal DW, Darling WG, Ge J, et al. Selective long-term reorganization of the corticospinal projection from the supplementary motor cortex following recovery from lateral motor cortex injury. *J Comp Neurol*. 2010;518(5):586-621. doi:10.1002/cne.22218
59. Morecraft RJ, Ge J, Stilwell-Morecraft KS, Rotella DL, Pizzimenti MA, Darling WG. Terminal organization of the corticospinal projection from the lateral premotor cortex to the cervical enlargement (C5–T1) in rhesus monkey. *J Comp Neurol*. 2019;527(16):2761-2789. doi:10.1002/cne.24706
60. Caggiano V, Sur M, Bizzi E. Rostro-caudal inhibition of hindlimb movements in the spinal cord of mice. *PLoS One*. 2014;9(6):e100865. doi:10.1371/journal.pone.0100865
61. Kitsikis A. The suppression of arm movements in monkeys: threshold variations of caudate nucleus stimulation. *Brain Res*. 1968;10(3):460-462. doi:10.1016/0006-8993(68)90216-3
62. Kitsikis A, Rougeul A. The effect of caudate stimulation on conditioned motor behavior in monkeys. *Physiol Behav*. 1968;3(6):831-837. doi:10.1016/0031-9384(68)90163-7
63. Jahanshahi M, Obeso I, Rothwell JC, Obeso JA. A fronto-striato-subthalamic-pallidal network for goal-directed and habitual inhibition. *Nat Rev Neurosci*. 2015;16(12):719-732. doi:10.1038/nrn4038
64. Aron AR, Herz DM, Brown P, Forstmann BU, Zaghloul K. Frontosubthalamic circuits for control of action and cognition. In: *Journal of Neuroscience*. Vol 36. Society for Neuroscience; 2016:11489-11495. doi:10.1523/JNEUROSCI.2348-16.2016
65. Schucht P, Moritz-Gasser S, Herbet G, Raabe A, Duffau H. Subcortical electrostimulation to identify network subserving motor control. *Hum Brain Mapp*. 2013;34(11):3023-3030. doi:10.1002/hbm.22122
66. Kinoshita M, de Champfleur NM, Deverdun J, Moritz-Gasser S, Herbet G, Duffau H. Role of fronto-striatal tract and frontal aslant tract in movement and speech: an axonal mapping study. *Brain Struct Funct*. 2015;220(6):3399-3412. doi:10.1007/s00429-014-0863-0
67. Côté SL, Hamadjida A, Quessy S, Dancause N. Contrasting modulatory effects from the dorsal and ventral premotor cortex on primary motor cortex outputs. *J Neurosci*. 2017;37(24):5960-5973. doi:10.1523/JNEUROSCI.0462-17.2017
68. Rosett J. *Intercortical Systems of the Human Cerebrum*. Columbia University Press; 1933. doi:10.7312/rose91600
69. Catani M, Dell'acqua F, Vergani F, et al. Short frontal lobe connections of the human brain. *Cortex*. 2012;48(2):273-291. doi:10.1016/j.cortex.2011.12.001
70. Guevara M, Román C, Houenou J, et al. Reproducibility of superficial white matter tracts using diffusion-weighted imaging tractography. *Neuroimage*. 2017;147:703-725. doi:10.1016/j.neuroimage.2016.11.066
71. Kirilina E, Helbling S, Morawski M, et al. Superficial white matter imaging: Contrast mechanisms and whole-brain in vivo mapping. *Sci Adv*. 2020;6(41):eaaz9281. doi:10.1126/sciadv.aaz9281
72. Simone L, Viganò L, Fornia L, et al. Distinct Functional and Structural Connectivity of the Human Hand-Knob Supported by Intraoperative Findings. *J Neurosci*. 2021;41(19):4223-4233. doi:10.1523/jneurosci.1574-20.2021
73. Howells H, Puglisi G, Leonetti A, et al. The role of left fronto-parietal tracts in hand selection: Evidence from neurosurgery. *Cortex*. 2020;128:297-311.

doi:10.1016/j.cortex.2020.03.018
74. Borra E, Luppino G. Large-scale temporo–parieto–frontal networks for motor and cognitive motor functions in the primate brain. *Cortex*. 2019;118:19-37. doi:10.1016/j.cortex.2018.09.024
75. Sani I, McPherson BC, Stemmann H, Pestilli F, Freiwald WA. Functionally defined white matter of the macaque monkey brain reveals a dorso-ventral attention network. *Elife*. 2019;8. doi:10.7554/eLife.40520
76. Ferbert A, Priori A, Rothwell JC, Day BL, Colebatch JG, Marsden CD. Interhemispheric inhibition of the human motor cortex. *J Physiol*. 1992;453(1):525-546. doi:10.1113/JPHYSIOL.1992.SP019243
77. Daskalakis ZJ, Christensen BK, Fitzgerald PB, Roshan L, Chen R. The mechanisms of interhemispheric inhibition in the human motor cortex. *J Physiol*. 2002;543(Pt 1):317. doi:10.1113/JPHYSIOL.2002.017673
78. Meyer B-U, Röricht S, Woiciechowsky C. Topography of fibers in the human corpus callosum mediating interhemispheric inhibition between the motor cortices. *Ann Neurol*. 1998;43(3):360-369. doi:10.1002/ANA.410430314
79. Makris N, Kennedy DN, McInerney S, et al. Segmentation of subcomponents within the superior longitudinal fascicle in humans: A quantitative, in vivo, DT-MRI study. *Cereb Cortex*. 2005;15(6):854-869. doi:10.1093/cercor/bhh186
80. de Schotten MT, Dell'Acqua F, Forkel SJ, et al. A lateralized brain network for visuospatial attention. *Nat Neurosci 2011 1410*. 2011;14(10):1245-1246. doi:10.1038/nn.2905
81. Kleist K. Gehirnpathologie. Published online 1934. Accessed May 5, 2021. https://psycnet.apa.org/record/1934-19904-001
82. Leiguarda RC, Marsden CD. Limb apraxias. Higher-order disorders of sensorimotor integration. *Brain*. 2000;123(5):860-879. doi:10.1093/brain/123.5.860
83. Fogassi L. Cortical mechanism for the visual guidance of hand grasping movements in the monkey: A reversible inactivation study. *Brain*. 2001;124(3):571-586. doi:10.1093/brain/124.3.571
84. Davare M, Andres M, Cosnard G, Thonnard J-L, Olivier E. Dissociating the role of ventral and dorsal premotor cortex in precision grasping. *J Neurosci*. 2006;26(8):2260-2268. doi:10.1523/JNEUROSCI.3386-05.2006
85. Naito E, Roland PE, Grefkes C, et al. Dominance of the Right Hemisphere and Role of Area 2 in Human Kinesthesia. *https://doi.org/101152/jn006372004*. 2005;93(2):1020-1034. doi:10.1152/JN.00637.2004
86. Naito E, Ehrsson HH. Somatic Sensation of Hand-Object Interactive Movement Is Associated with Activity in the Left Inferior Parietal Cortex. *J Neurosci*. 2006;26(14):3783-3790. doi:10.1523/JNEUROSCI.4835-05.2006
87. Gerbella M, Borra E, Mangiaracina C, Rozzi S, Luppino G. Corticostriate projections from areas of the "lateral grasping network": Evidence for multiple hand-related input channels. *Cereb Cortex*. 2016;26(7):3096-3115. doi:10.1093/cercor/bhv135
88. Catani M, Mesulam MM, Jakobsen E, et al. A novel frontal pathway underlies verbal fluency in primary progressive aphasia. *Brain*. 2013;136(8):2619-2628. doi:10.1093/brain/awt163
89. Rizio AA, Diaz MT. Language, aging, and cognition: Frontal aslant tract and superior longitudinal fasciculus contribute toward working memory performance in older adults. *Neuroreport*. 2016;27(9):689-693. doi:10.1097/WNR.0000000000000597
90. Budisavljevic S, Dell'Acqua F, Djordjilovic V, Miotto D, Motta R, Castiello U. The role of the frontal aslant tract and premotor connections in visually guided hand movements. *Neuroimage*. 2017;146:419-428. doi:10.1016/j.neuroimage.2016.10.051

91. Krainik A, Lehéricy S, Duffau H, et al. Role of the supplementary motor area in motor deficit following medial frontal lobe surgery. *Neurology*. 2001;57(5):871-878. doi:10.1212/WNL.57.5.871
92. Schulz R, Braass H, Liuzzi G, et al. White matter integrity of premotor-motor connections is associated with motor output in chronic stroke patients. *NeuroImage Clin*. 2015;7:82-86. doi:10.1016/j.nicl.2014.11.006
93. Boccuni L, Meyer S, D'cruz N, et al. Premotor dorsal white matter integrity for the prediction of upper limb motor impairment after stroke. *Sci Rep*. 2019;9(1):1-9. doi:10.1038/s41598-019-56334-w
94. Rizzi M, Sartori I, Vecchio M Del, et al. Tracing in Vivo the Dorsal Loop of the Optic Radiation: Convergent Perspectives From Tractography and Electrophysiology Compared to a Neuroanatomical Ground Truth. *Res Sq [Preprint]*. Published online June 10, 2021. doi:10.21203/RS.3.RS-589114/V1

Figure legends

Figure 1. **Study flowchart**

Figure 2. **Intraoperative hand manipulation task (HMt):** (A) Representation of the hand manipulation task used in the intraoperative setting, and exemplificative Abductor pollicis brevis EMG pattern (APB; raw signal in black, rectified signal in red) during baseline execution of the task (B). The window between green vertical dashed lines indicates the time used to shape the fingers immediately before the contact with the object, to grasp it, to rotate it and turning back to the initial shaping phase. (C) The common tested area in all patients in the frontal lobe, shown normalised to the MNI template on axial slices.

Figure 3: **Anatomically segregated effects of DES on object manipulation using EMG pattern analysis: (A)** Abductor pollicis brevis activity (APB; raw signal in black, rectified signal in red) during an arrest pattern (left, in orange) and a clumsy pattern (right, in blue). The orange and blue shadows represent the onset and offset of stimulations. (B-C) Distribution of stimulation sites in right and left hemisphere based on aCC value (orange = arrest pattern; blue = clumsy pattern) normalised to the MNI template. (D-E) Probability density estimation of EMG-interference patterns (arrest pattern in orange, clumsy in blue) shown on a right and left 3D white matter MNI reconstruction and on coronal MNI slices.

Figure 4. **Disconnectome maps associated with EMG-interference patterns**. Statistical disconnectome maps (TFCE, p-fwer <0.05) predicting the arrest pattern (red) or the clumsy pattern (blue) shown on normalised axial slices in the right (A) and left (B) hemisphere. Percentage of overlap between the statistical disconnectome maps and white matter tracts from a healthy population atlas (Yeh et al. 2018) in the right (C) and left (D) hemisphere (callosal fibres not shown). 3D renderings of the right and left disconnectome maps (E). On axial slices is shown the overlap between the disconnectome maps and both corticospinal (F) and striatal fibres (H). The sagittal slices show the overlap between the disconnectome maps and the association tracts (G).

Figure 5. **White matter tracts associated with different stimulation effects – single subject diffusion tractography**. (A) Bar graph shows the percentage of stimulations, within tract, producing the arrest or the clumsy pattern. (B) Bar graph shows the total number of

stimulations for each tract. All tracts are represented on normalised templates, divided based on their likelihood to be associated with arrest pattern (C) or clumsy pattern (D). The FAT was associated to both effects (E). The lower panel shows a single patient who underwent surgery for a right frontal anaplastic oligodendroglioma (grade III) who did not experience a postoperative deficit. Screenshot from surgical video taken during subcortical stimulation and corresponding EMG interference patterns are reported for multiple sites. Arrest pattern was elicited in site 1 (F, aCC = 0, RMS = 45% compared to baseline) and in site 2 (H, aCC = 0, RMS = 31% compared to baseline). Clumsy pattern was elicited in site 3 (I, aCC = 0.3, RMS = 45% compared to baseline) and in site 4 (J, aCC = 0.9, RMS = 69% compared to baseline). These sites are shown relative to the underlying white matter anatomy of the patient (G), traced using diffusion tractography. Resection cavity (dark grey) and tumour (light grey) are overlaid in the same space.

Figure 6. **Effect of resection on immediate post-operative motor outcome.** (A) Overlap maps of resection cavities of all patients. (B) Significative cluster associated with a decrease in upper-limb motor performance (5 days post-surgery, MRC score). This cluster is also displayed in 3D reconstructions showing its overlapping with the projection fibres from the SMA and the Sup-FST (C, D). (E) Percentage of streamlines disconnected by the neurosurgical procedure for each tract in the 15 patients with tractography. Motor outcome is compared between the three patients with transient MRC deficit (red) and those without deficits (blue).

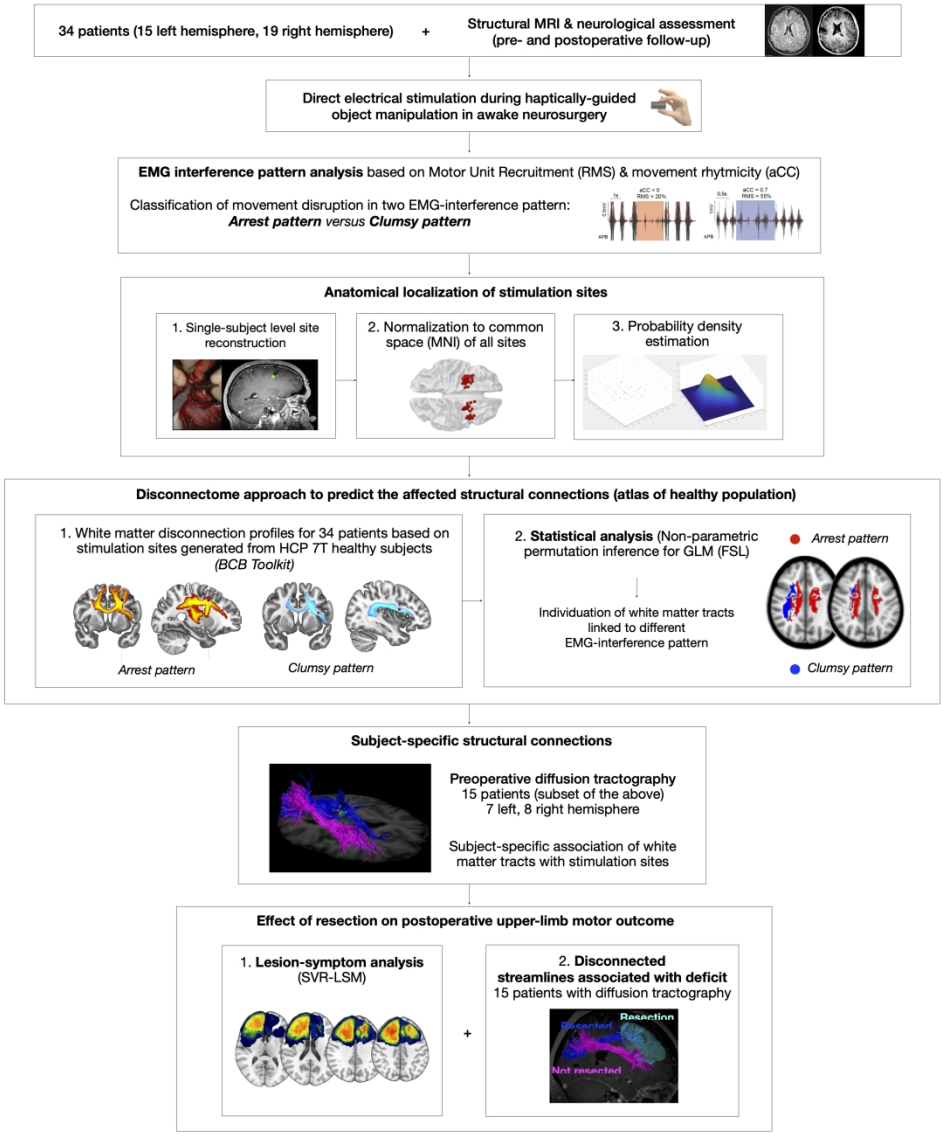

Figure 1

280x323mm (300 x 300 DPI)

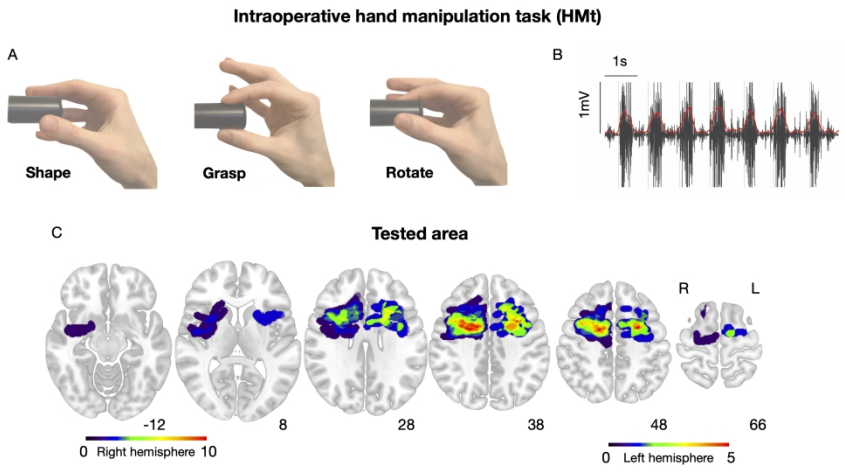

Figure 2

281x133mm (300 x 300 DPI)

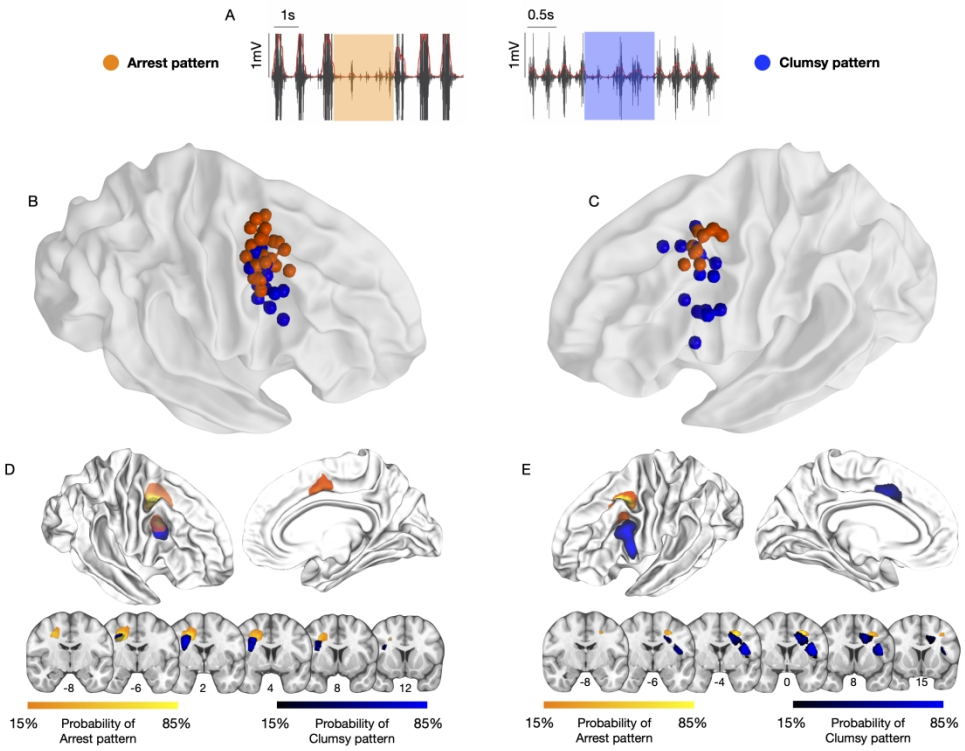

Figure 3

281x212mm (300 x 300 DPI)

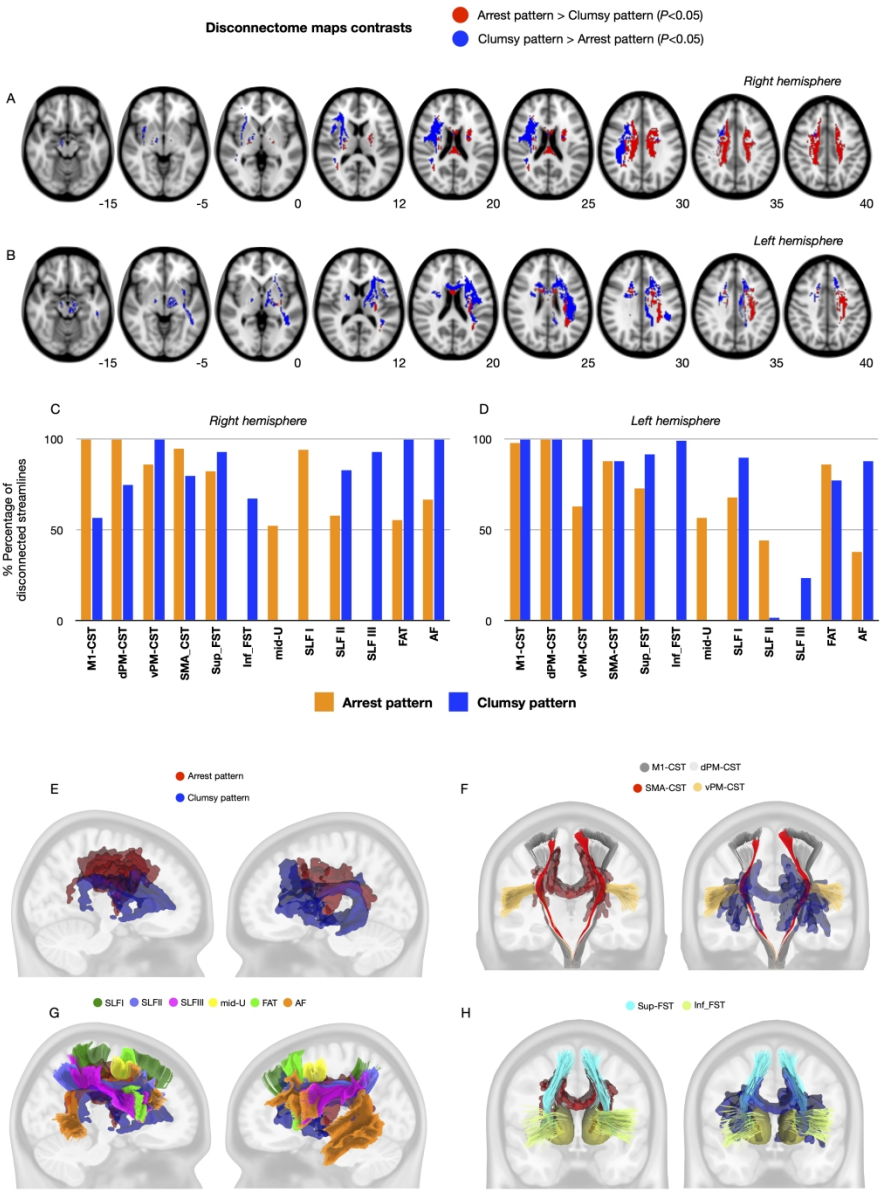

Figure 4

280x373mm (300 x 300 DPI)

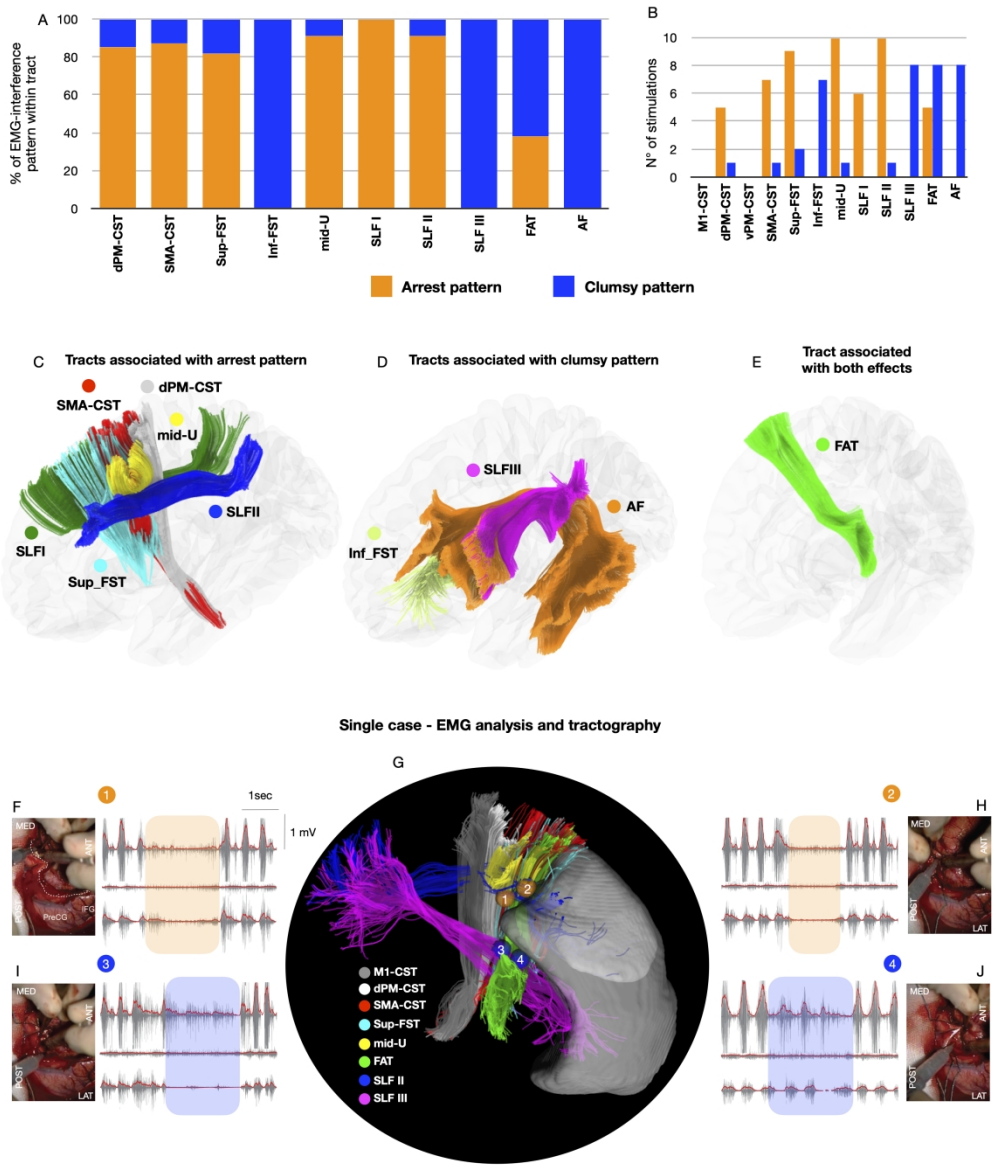

Figure 5

281x331mm (300 x 300 DPI)

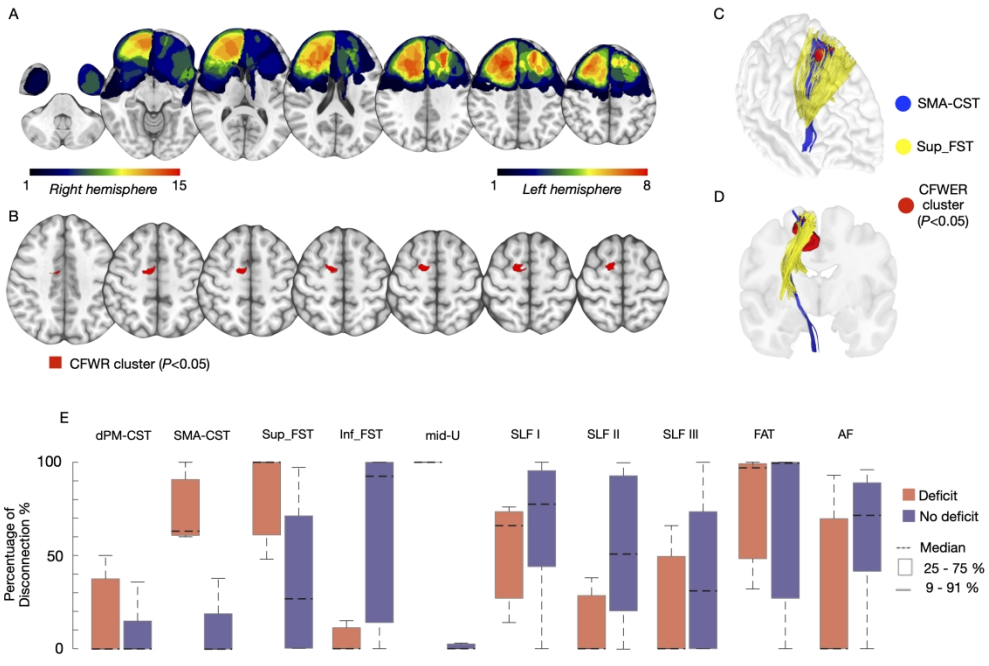

Figure 6

281x188mm (300 x 300 DPI)

Table 1 Demographic and clinical information on the entire sample

Patient no	Hem	Histology	Grade	Eor	Sex	Age	Handedness	5-day MRC scale	De Renzi score
1	Right	Astrocytoma	III	supratotal	M	43	R	2 (SMA-syndrome)	n.a.
2	Right	Anaplastic astrocytoma	III	supratotal	M	59	R	5	3
3	Right	Oligodendroglioma	II	supratotal	M	29	R	5	3
4	Left	Glioblastoma	IV	total	F	64	R	5	3
5	Left	Anaplastic oligodendroglioma	III	supratotal	F	46	R	5	3
6	Right	Astrocytoma	II	supratotal	M	27	R	5	3
7	Left	Oligodendroglioma	III	total	M	45	R	5	3
8	Right	Astrocytoma	II	supratotal	F	35	R	5	3
9	Left	Oligodendroglioma	II	supratotal	F	38	R	5	2
10	Right	Anaplastic oligodendroglioma	III	total	F	54	R	5	3
11	Left	Glioblastoma	IV	total	M	54	R	5	3
12	Left	Glioblastoma	IV	total	M	38	R	3	n.a.
13	Left	Neurocytoma	II	total	M	38	R	2 (SMA-syndrome)	n.a.
14	Right	Oligoastrocytoma	II	supratotal	F	22	R	2 (SMA-syndrome)	3
15	Right	Anaplastic astrocytoma	III	supratotal	M	38	R	5	3
16	Left	Oligodendroglioma	II	supratotal	M	38	R	5	3
17	Right	Glioblastoma	IV	total	F	39	R	2	n.a.
18	Right	Oligodendroglioma	II	supratotal	F	22	R	3	n.a.
19	Right	Oligodendroglioma	II	supratotal	F	34	R	2 (SMA-syndrome)	n.a.
20(a)	Right	Astrocytoma	II	total	F	42	R	3	n.a.
21(a)	Left	Oligodendroglioma	II	total	M	41	L	5	3
22(a)	Left	Oligodendroglioma	III	supratotal	F	55	R	5	3
23(a)	Right	Oligodendroglioma	II	supratotal	M	31	R	5	3
24(a)	Right	Anaplastic astrocytoma	III	supratotal	M	28	L	5	2
25(a)	Right	Oligoastrocytoma	III	supratotal	F	49	R	2	n.a.
26(a)	Left	Astrocytoma	III	supratotal	F	40	R	5	3
27(a)	Right	Oligodendroglioma	II	supratotal	M	45	L	5	3
28(a)	Right	Astrocytoma	II	supratotal	F	29	R	5	3
29(a)	Left	Glioblastoma	IV	supratotal	F	34	L	5	3
30(a)	Right	Anaplastic astrocytoma	III	total	F	53	R	5	3
31(a)	Left	Astrocytoma	II	supratotal	F	57	R	2	n.a.
32(a)	Left	Glioblastoma	IV	total	M	54	R	5	3
33(a)	Left	Anaplastic astrocytoma	III	supratotal	M	40	R	5	3
34(a)	Right	Astrocytoma	II	supratotal	M	47	R	5	3

Note: (Hem) refers to Hemisphere; (Eor) refers to extent of resection; (a) refers to patients that underwent diffusion MR imaging for tractography. F: female; M: male; De Renzi score: 3 (>62); 2 (53-62); 1 (<53); n.a.: not administrated.

Table 2 Tract measurements for the 15 patients with diffusion tractography

No	Hem	M1-CST	dPM-CST	vPM-CST	SMA-CST	Sup-FST	Inf-FST	mid-U	SLFI	SLFII	SLFIII	FAT	AF
20	R	5.5	3.4a	1.6	8.5a	11.4a	0.56	1.52a	22.1a	8.691a	17.1	7.4a	3.23
21	L	8.3	5.5	5.1	10.3a	10.1a	1.6	2.46a	17.1	22.6a	15.4	19.1a	8.9
22	L	11.7	4.2a	2.9	7.7a	2.8a	3.3c	6.1a	9.0a	9.34	11.1c	4.2a,c	9.6c
23	R	4	3.9a	2.8	7.6a,c	4.39a,c	3.03c	9.2a,c	18.9	21.8a,c	20.3c	1.6c	7.9c
24	R	8.6	4.3a	0.4	9.1	8.3a,c	11.1	2.6a	19.8	10.2a	21.7c	11.5c	10.9c
25	R	6.1	2	2.7	10.1a	4.9a	11.4	13.2a	26.3a	16.3a	25.4	9.2	5.6
26	L	6	5.4	0.4	10.6	4.7	0.4	6.1a	13.1a	13.6a	24.5	6.7	15.2
27	R	4.3	4.5	0.4	12.3a	6.2a	3.2c	5.2	25.6a	27.6a	19.5c	8.35a,c	9.4c
28	R	5.4	4.4	2.3	6.6	2.8	5.4	4.1a	28.2	21.1a	27.3	11.9	10.9
29	L	7.5	5.9	0.8	7	2.9	3.1c	2.4	21.9	19.9	8.6c	9.8c	3.9c
30	R	4.7	3.7	9.1	8.9	0.5	10.1c	2.4	22.5	17.5	19.3c	8.3	9.9c
31	L	5.8	4	2.4	5.7a	2.4a	1.6	6.3a	12.8a	9.7a	15.4	17.8a	8.9
32	L	8.2	4.2	2.9	10.7	3.9	1.8c	4.2	18.5	19.2	12.4c	12.3c	18.5c
33	L	3.7	1.4	3.9	4.9	1.9	12.3c	8.3	22.2	10.8	26.1c	9.5c	24.6c
34	R	15.6	8.4a,c	4	7.5	0.8a	5.2	3.13a	32.03	19.2a	16.7	12.3c	5.11

Note: (a) refers to arrest pattern, while (c) to clumsy pattern. M1-CST: primary motor area corticospinal tract; dPM-CST: dorsal premotor area corticospinal tract; vPM-CST: ventral premotor area corticospinal tract; SMA-CST: supplementary motor area corticospinal tract; Sup_FST: superior fronto-striatal tract; Inf_FST: inferior fronto-striatal tract; mid-U: local U-shaped connections between the precentral gyrus and the middle frontal gyrus; SLF: superior longitudinal fasciculus I, II and III; FAT: frontal aslant tract; AF: arcuate fasciculus. Measurements are expressed in ml.